



Morphological and molecular criteria allow the identification of putative germ stem cells in a lophotrochozoan, the Pacific oyster *Crassostrea gigas*

Maëva Cherif-Feildel^{1,2} · Kristell Kellner^{1,2} · Didier Goux^{1,3} · Nicolas Elie^{1,3} · Béatrice Adeline^{1,2} · Christophe Lelong^{1,2} · Clothilde Heude Berthelin^{1,2}

Accepted: 6 October 2018
© Springer-Verlag GmbH Germany, part of Springer Nature 2018

Abstract

While our knowledge of bivalve gametogenesis recently progressed, data on early stages of gametogenesis remain to be developed, especially when dealing with germinal stem cells (GSC) and their niche in these organisms. Here, we wish to develop a strategy to identify putative GSC in Pacific oyster *Crassostrea gigas* based on morphological criteria combined with vasa marker expression. A histological quantitative approach, based on stereology, allowed us to identify two types of early germ cells in the germinal epithelium, one presenting round nuclei and the other irregular ones. Both early germ cell types present slightly condensed chromatin in nucleus, are vasa-positive and the *Oyvlg* (oyster vasa-like gene) expression in these cells is recorded throughout the whole gametogenesis process. The microenvironment of an early germ cell in oyster includes an associated somatic cell presenting an immunolabeling for BMP2/4 and a close myoid cell. In agreement with the GSC characteristics in other species, we postulate that putative germ stem cells in *C. gigas* correspond to the early germ cell type with irregular nucleus shape; those early germ cells with a round nucleus may consist in progenitors.

Keywords Germinal stem cell · Germinal niche · Lophotrochozoans · *Crassostrea gigas* · Quantitative histology · Vasa

Introduction

Reproduction ensures the sustainability of a species, it presents much diversified processes but the earliest stages of gametogenesis are well conserved among species. It is of the utmost importance to know the characteristics and functioning of GSC in an organism to understand the regulation of these early stages of gametogenesis. There is only few data

available on GSC and their microenvironment in lophotrochozoans. In terms of development, organization and physiology, lophotrochozoans differ largely from the two other major phylogenetic clades of bilaterian animals (Adoutte et al. 2000). However, their relatively simple organization and their ancestral position in phylogenetic trees make them an interesting case to study in terms of evolutive and fundamental biology.

Among lophotrochozoans, in phylum of Platyhelminths, planarian stem cells were widely studied and some remarkable adult stem cells named neoblasts could be described in these flatworms. These cells are pluripotent cells by nature and are able to differentiate between all zygotic cell types included somatic and germ cells (Rossi et al. 2008; Bagnù 2012; Rink 2013). These organisms present asexual and sexual reproduction modes, depending on the species. To enhance our understanding of GSC nature in lophotrochozoans, studying a species exempt of asexual reproduction mode is particularly interesting. The oyster *Crassostrea gigas* reproduces only by sexual reproduction mode and presents an annual reproductive cycle. In this alternative hermaphrodite, germ and somatic lines present in the gonad may be

Electronic supplementary material The online version of this article (<https://doi.org/10.1007/s00418-018-1740-3>) contains supplementary material, which is available to authorized users.

✉ Clothilde Heude Berthelin
clothilde.heude@unicaen.fr

¹ Normandy University, Caen, France

² Université de Caen Normandie, Unité mixte de recherche Biologie des Organismes et Ecosystèmes Aquatiques MNHN, Sorbonne Université, UCN, CNRS-7208, IRD-207, UA, Caen, France

³ Université de Caen Normandie, UNICAEN, SF 4206 ICORE, CMABIO3, 14000 Caen, France

male or female lines depending on the adult reproductive cycle. Gonadal tubules embedded in a dense conjunctive tissue specialized in glycogen storage form the gonad located between the visceral mass and the mantle (Berthelin et al. 2000a, b). The course of gametogenesis as well as the gonad structure have been described (Steele and Mulcahy 1999; Heude Berthelin et al. 2001; Franco et al. 2008).

Each year, the storage tissue redevelops at the time of the first gonial mitosis, and then development of germline leads to a progressive regression of the storage tissue. At the end of each gametogenetic cycle, after the emission of gametes, the storage tissue is broadly depleted and gonadal tubules appear almost empty (Berthelin et al. 2000a). Different stages of gametogenesis are described in this species (Heude Berthelin et al. 2001; Franco et al. 2008). At the quiescent stage (stage 0) the early germ cells present in the tubules are not sufficiently differentiated to allow sex identification and no mitotic activity is noted. The early development of germinal epithelium (stage 1) is characterised by the beginning of the gonial proliferation. During the stage 2 of gametogenesis, all the germ cell types are observed in the germinal epithelium with a minor proportion of mature gametes. The last stage of gametogenesis (stage 3) corresponds to the mature reproductive stage where mature gametes constitute the majority of the germ cells present in the tubules.

Recent sequencing of the genome of *C. gigas* (Zhang et al. 2015) and the availability of several transcriptomes (Dheilly et al. 2012; Zhang et al. 2012; Zhao et al. 2012) give access to stem cell putative markers which are also helpful to localize and characterize GSC in this species. Markers of stemness are usually used in histochemistry and immunochemistry approaches to identify the GSC. Recent publication of Cavelier et al. (2017) reports alkaline phosphatase activity in germ cells localized in outer genital *C. gigas* gonad ducts. The dynamics of stem cells was also classically investigated using BrdU or phosphorylated-histone H3 labelling to detect quiescence or reduced rate of proliferation (Newmark and Alvarado 2000; Jemaà et al. 2014). The expression measurement of specific and conserved markers of germ stemness, among bilaterians (Vasa, Nanos, Piwi for example) was also commonly used to localize GSC (Juliano et al. 2010; Brown and Swalla 2012; Maceren-Pates et al. 2015). In particular, Vasa, an evolutionary conserved DEAD-box RNA helicase that plays different functions in germ cell formation and germline maintenance is one of evolutionarily conserved germ cell marker (reviewed in Lasko 2013) therefore, GSC. In *C. gigas*, it has recently been shown that the nanos transcript was detected in early germinal cells and the authors suggested its implication in the differentiation of cells with stem cell-like properties (Xu et al. 2018). In the oyster and more broadly in bivalves, Vasa is for the moment the only one marker of germ cells at the protein level. Fabioux et al. (2004b) showed that, in the particular

case of oyster *C. gigas*, the vasa-like gene (*Oyvlg*) is specifically expressed in gonad tissue as well as the protein (Fabioux et al. 2009) but the cellular location of this protein was not investigated. More recently, Cavelier et al. (2017) identified Vasa-positive germ cells in gonad ducts in the earliest stages of gametogenesis. Likewise, Obata et al. (2010) detected Vasa-positive cells in the *Mytilus galloprovincialis* mussel and Milani et al. (2015, 2017) confirmed by immunodetection that Vasa is a germ cell marker in several bivalve species. The morphological criteria of stem cells are also commonly used for GSC identification as elevated nucleocytoplasmic ratio, slightly condensed chromatin, the presence of a nuage in the cytoplasm, associated with numerous and round mitochondria (Chiarini-Garcia and Russell 2001, 2002). In *C. gigas*, Franco et al. (2008) described an early spermatogonia type; however, for the time being, the germ stem cell at the origin of both male and female germlines in this alternative hermaphrodite are neither identified nor described. Stereological approach is applied to characterize cell types or structural changes in cells fields such neurology (Schmitz and Hof 2005; Golub et al. 2015), cancer cell biology (Ladekarl 1998; Meijer et al. 1998) and reproductive biology (Johnson et al. 2008; Silva et al. 2010). The stereological approach allows investigating a large number of samples from a routine technique like histology. Stereology is based on the principles of geometry and statistics and provides an unbiased quantitative tool allowing access to estimation of 3D parameters based on the structures of 2D sections (Garcia et al. 2007; Brown 2017). This method could be of interest to investigate GSC identity in *C. gigas*.

GSC commonly reside in a special microenvironment, termed germinal niche, provided by somatic support cells, in which they both self-renew and produce progenitors that start the differentiation process while leaving the niche (for review see Spradling et al. 2011). Some elements of the niche appear conserved in the protostomes (Lophotrochozoa and Ecdysozoa) and in deuterostomes as the extracellular matrix which supports the stem cells, some associated somatic cells and myoid cells and a nervous network (Scadden 2006; Ferraro et al. 2010).

The different actors of the niche integrate several molecular signals to ensure functional and structural roles in stem cells destiny. This particular microenvironment controls the stem cells stock by the regulation of their properties of proliferation, auto-renewal and differentiation (Scadden 2006; Morrison and Spradling 2008). These mechanisms are controlled by different signaling pathways as Wnt/ β -catenin, Notch, insulin and Transforming Growth Factors β (TGF- β) (Ferraro et al. 2010). TGF- β (activins and Bone Morphogenetic Proteins BMP), are particularly involved in the control of cell proliferation and in the maintenance of stem cells in numerous species. In *C. gigas*, previous findings demonstrated the occurrence of a diversity of TGF- β signaling

components including various ligands and two subfamilies of receptors: type I receptors, type II BMP/activin, and most of the Smad downstream transducers (Herpin et al. 2004, 2005; Le Quere et al. 2009). Oyster-gonadal-TGF- β (og-TGF- β) was classified as a derived member of the TGF- β superfamily (Fleury et al. 2008). According to the authors, its expression appeared to be gonad-specific and located in associated somatic cells surrounding the germ cells in both male and female. The *in vivo* og-TGF- β dsRNA injection into the oyster's gonad, when injected at the initiation of gametogenesis, leads to a reduction of the number of germ cells in both male and female (Huvet et al. 2012). Among identified ligands in oyster, *Crassostrea gigas*-Glass bottom boat (Cg-Gbb) was found to present a homology with Gbb of *drosophila* as well as with the human Bone Morphogenetic Protein 8 (BMP8). Cg-mGDF, a homologous of the *drosophila* Decapentaplegic (Dpp) and of the human BMP2/4, is also conserved in *C. gigas*. This ligand in *drosophila* is essential for the regulation of germ stem cells stock in the gonad (Xie and Spradling 1998) and is expressed by somatic cells in the germinal niche in male and female (Jagut and Huynh 2007).

Here, we report an original approach to locate and characterize putative GSC in a sexually reproducing lophotrochozoan organism, the Pacific oyster *Crassostrea gigas*. To identify putative GSC we used a histological quantitative approach based on morphological criteria of GSC combined with the detection of Vasa-positive germ cells in the gonad. Microenvironment of identified putative GSC was also specified using an anti-BMP2/4 antibody.

Materials and methods

Animals

Pacific oysters (*Crassostrea gigas*, 2 years old) were provided by a commercial oyster farm in Saint-Vaast la Hougue (Manche, France). Every 2 months, 30 diploid oysters were sampled. Ploidy was individually verified on gill tissue samples according to the protocol set up by Jouaux et al. (2010).

Light microscopy

Transverse sections were fixed for histology in Davidson's fixative at 4 °C (10% glycerol, 20% formaldehyde, 30% ethanol 95°, 30% sterile seawater, 10% acetic acid) for 48 h. The tissue samples were dehydrated in successive dilutions of ethanol, then transferred in butanol (Carlo Erba, France) and embedded in paraffin wax (Roth, France). Three micrometers sections were stained according to the Prenant-Gabe trichrome or Feulgen staining protocols (Gabe 1968). The

stages of the gametogenetic cycle were individually determined according to Heude Berthelin et al. (2001).

Quantitative histology

The quantitative histological approach consists of two steps (online resource 1). The first step consisted in selecting three animals at each stage of male and female gametogenesis, and each corresponding slide was treated according to the Feulgen staining protocol (Gabe 1968). Each slide was used to photograph a series of 25 fields (objective 100) dispatched on the whole gonadal area using a Nikon eclipse 80i microscope and a Nikon DS-Ri2 camera with the Nikon software. According to the literature, the fields were chosen along the gonad tubule wall to reveal the preferential location of GSC. The nucleus located along the tubule wall and exhibiting a slightly condensed chromatin (stemness criteria) were measured by line-intercept sampling according to the method described by Gundersen and Jensen (1985). Thanks to computer program designed to automate measurement of targeted cells, a total of 196,149 cells were measured for the whole set of gametogenetic stages studied in this first step. A stereological estimation of the volume-weighted mean volume was thus calculated using the Cruz-Orive and Hunziker (1986) ruler for each stage and sex. The second step in the histological quantitative study on the selected Feulgen stained slides consisted in the measurement of an ellipse surrounding each nucleus of interest for computer calculations of the longest and the shortest diameters. A total of 1410 cells were measured for the second step after Feulgen staining. The calculation of elongation ratios, consisting in dividing the shortest diameter by the longest diameter, gives an accurate idea of the nucleus shape (round nucleus > 0.8 , irregular nucleus ≤ 0.8). The elongation ratios were also calculated for Oyvlg positive cells after immunolabelling for one selected slide for each gametogenesis stage. A total of 952 cells were measured for the second step after Oyvlg immunolabelling. All measures were performed using Fiji software. The reproducibility of the measurements was evaluated by measuring all the cells of one field (10 cells), 10 times each, and no significant difference was observed in the variance (variance test, $\alpha = 0.05$). The coefficient of variation was calculated on the basis of these measurements, by dividing the standard deviation by the mean.

Whole Slide Image (WSI) was obtained using an Aperio scanner (magnification 40 \times) and nuclei of interest were spotted using QuPath software (Bankhead et al. 2017).

Oyvlg antibody

Anti-Oyvlg antibody was kindly provided by C. Fabioux (UBO, France) and C. Corporeau (Ifremer, France). This rabbit polyclonal antibody, produced by Millegen (Labege,

France), targeted two peptides (GSKNDGESSGFGGG and EEGHFARECPEPRK) specific of the Oyvlg amino acid sequence. The specificity of this antibody in oyster gonad was attested in Fabioux et al. (2009).

Immunohistochemistry

Three and ten-micrometer sections were deparaffinized for immunolabelling and immunofluorescence procedures, respectively. Immunolabelling was performed according to Franco et al.'s indications (2010). Control without primary or secondary antibodies were performed. Rabbit polyclonal primary antibodies, anti-BMP2/4 (sc-9003, Santa Cruz Biotechnology, USA) and anti-Oyvlg were diluted at 1:50 and 1:500, respectively. For anti-BMP2/4, antigen retrieval was done by immersing the sections in saponine 0.05% for 30 min. The secondary antibody used was the horseradish-peroxidase conjugated polyclonal swine anti-rabbit Immunoglobulins (P0399, Dako Agilent Technologies, USA) diluted at 1:100. For immunofluorescence labelling with Oyvlg, rehydrated sections were incubated in 3% H₂O₂/PBS (500 mM NaCl, 10 mM Na₂HPO₄, 3.1 mM KH₂PO₄, pH 7.4) overnight at 4 °C as prescribed by Chong et al. (2011). The sections were washed with PBS and incubated in the saturation solution (10% normal goat serum, 0.25% BSA, 1% Triton X-100) for 1 h at 4 °C. The Oyvlg antibody, diluted at 1:500 in the saturation solution, was dropped on the incubated sections overnight at 4 °C. The sections were washed and incubated with the donkey anti-rabbit IgG secondary antibody Alexa Fluor[®] 488 conjugate (A-21,206, Thermo Fisher Scientific, France) diluted 1:1000 in PBS for 2 h at room temperature. The sections were washed in PBS and mounted in Vectashield[®] with DAPI. Immunolabelling were repeated at least three times. The photographs in light microscopy were obtained using a Nikon eclipse 80i microscope and a Nikon DS-Ri2 camera with the Nikon software and those in fluorescence were obtained using the Olympus FLUOVIEW FV1000 confocal laser scanning microscope and the Olympus software FV10-ASW 4.2. Image processing was done using Fiji software.

RNA probe synthesis

Digoxigenin-labelled RNA probes were synthesized from the clone of an oyvlg fragment (1745 bp) by PCR using a cDNA library normalized to all tissues and developmental stages of *C. gigas* and specific primers (Forward: 5'-ACGTGCGTA AAGCCAGTAT-3' and Reverse: 5'-CAATCCGCCGAA CATTACTT-3'). RNA probes were labelled using the DIG RNA labelling kit (SP6/T7) (Roche) as recommended by Fabioux et al. (2004b).

In situ hybridization (ISH)

Three-micrometer sections mounted on Superfrost Ultra Plus slides were heated overnight at 37 °C, 2 min at 56 °C and 30 min at room temperature before dewaxing and rehydration in serial ethanol dilutions. The sections were treated with Proteinase K (5 µg/mL in Tris-EDTA Buffer pH 8) for 5 min and rinsed in PBS. Post-fixation in PBS/PFA 4% (7 min) was done before rinsing in PBS (3 min) and in 2X SSC (2×5 min). The sections were pre-hybridized for 60 min at 50 °C in hybridization buffer (4X SSC, 10% dextran sulfate, 1X Denhardt's solution, 2 mM EDTA, 50% deionized formamide, 500 µg/mL salmon genomic DNA) before the hybridization step with 200 ng/mL of RNA probes in hybridization buffer overnight at 50 °C. Sections were rinsed in 2X SSC (5 min) and treated with 60% formamide in 0.2X SSC (3×5 min), at 55 °C before rinses in 2X SSC (2×5 min) and in 100 mM Tris-HCl pH 7.5 with 150 mM NaCl (5 min) at room temperature. The slides were then treated for 30 min with blocking buffer (100 mM Tris-HCl pH 7.5, 150 mM NaCl, 1% blocking reagent) before incubation with the alkaline phosphatase-conjugated anti-DIG antibody (polyclonal, Fab fragments) diluted 1:2000 in blocking buffer. Rinses were performed with 100 mM Tris-HCl, 150 mM NaCl (2×5 min) and with detecting buffer (100 mM Tris-HCl pH 9.5, 100 mM NaCl, 50 mM MgCl₂, 10 min). An overnight incubation with a BCIP/NBT STOCK solution diluted at 1:50 and a rinsing process in Tris-EDTA buffer (5 min) were done. Dehydration was made in 100% ethanol (2×1 min) and in Roti-Histol (5 min) before mounting. Negative controls were performed with sense probes. ISH was performed in triplicates.

RNA extraction and cDNA synthesis

For each of the gametogenesis stages, four pools of three gonadal area samples were done. Tissues were ground in 1 mL of TriReagent at room temperature (Sigma Aldrich, France). One hundred microliters of 1-Bromo-3-chloropropane (Sigma Aldrich, France) were added and samples were vortexed before a 15 min centrifugation at 4 °C. The aqueous phase was recovered and the total RNA extraction was performed using Nucleospin RNA II kit (Macherey-Nagel). The RNA samples were reverse transcribed as recommended by Dheilly et al. (2012).

Real-time polymerase chain reaction

The primers sequences for Oyvlg (Forward: 5'-CACAAG TCAGACCGAGTGCA-3' and Reverse: 5'-GCGATG GTGTGATGATTGGC-3') and EF1α (Forward: 5'-ACG ACGATCGCATTCTCTT-3' and Reverse: 5'-ACCACC CTGGTGAGATCAAG-3') were designed using Primer3

software and folding analysis (<http://unafold.rna.albany.edu/?q=mfold>). Quantitative PCR were done using 1X GoTaq SYBR Green Mix (Promega, France), 8.85 ng cDNA and 900 nM of each primer in a final volume of 15 μ L. Each run consisted of one cycle of 5 min at 95 °C followed by 45 cycles of 15 s at 95 °C and 45 s at 60 °C. Specific amplification of the target sequence was estimated by constructing melting curves (80 cycles of 10 s, increasing the temperature by 0.5 °C step from 55 °C to 95 °C). The reference gene (EF1 α) was selected among the three tested housekeeping genes (GAPDH, Arf1, EF1 α) after the checking of constant expression and in agreement with previous studies using the same tissues and species (Fabioux et al. 2009; Dheilly et al. 2011; Dubos et al. 2016).

Electron microscopy

Small pieces of gonadal area tissue were sampled and immersed for 16 h at 4 °C in a fixative solution (2.5% glutaraldehyde, 0.31 M cacodylate, 0.25 M saccharose, pH 7.4). The samples were rinsed in 0.38 M cacodylate buffer with 0.28 M saccharose at 4 °C and post-fixed for 2 h with 1% osmium tetroxide in 0.2 M cacodylate buffer containing 0.365 M saccharose. Tissues were dehydrated in ascending acetone concentrations and embedded in Epon. Ultrathin sections were mounted on coated copper grids and contrasted with uranyl acetate followed by lead citrate. Ultrathin sections were examined with a JEOL1011 transmission electron microscope. Image processing was done using Fiji software.

Statistical analysis

Statistical analyses were performed using a variance test and a non-parametric one-way analysis with permutation test on R 3.4.3 and RStudio software ($\alpha=0.05$).

Results

Quantitative histology

The first step of the histological quantitative approach allowed us to obtain the volume-weighted mean volume of germ cells nuclei which we wish to focus on here (early germ cells) at each stage of the gametogenesis (Fig. 1a). It appeared that most of the stages of the gametogenesis shared some common nucleus volumes (range between 76.91 and 97.67 μ m³). This common population of early germ cells was found in four of the seven stages of the gametogenesis (no significant difference): in the quiescence stage (St0), the male gonial mitosis initiation stage (St1M), the female germline development stage (St2F) and the female sexual

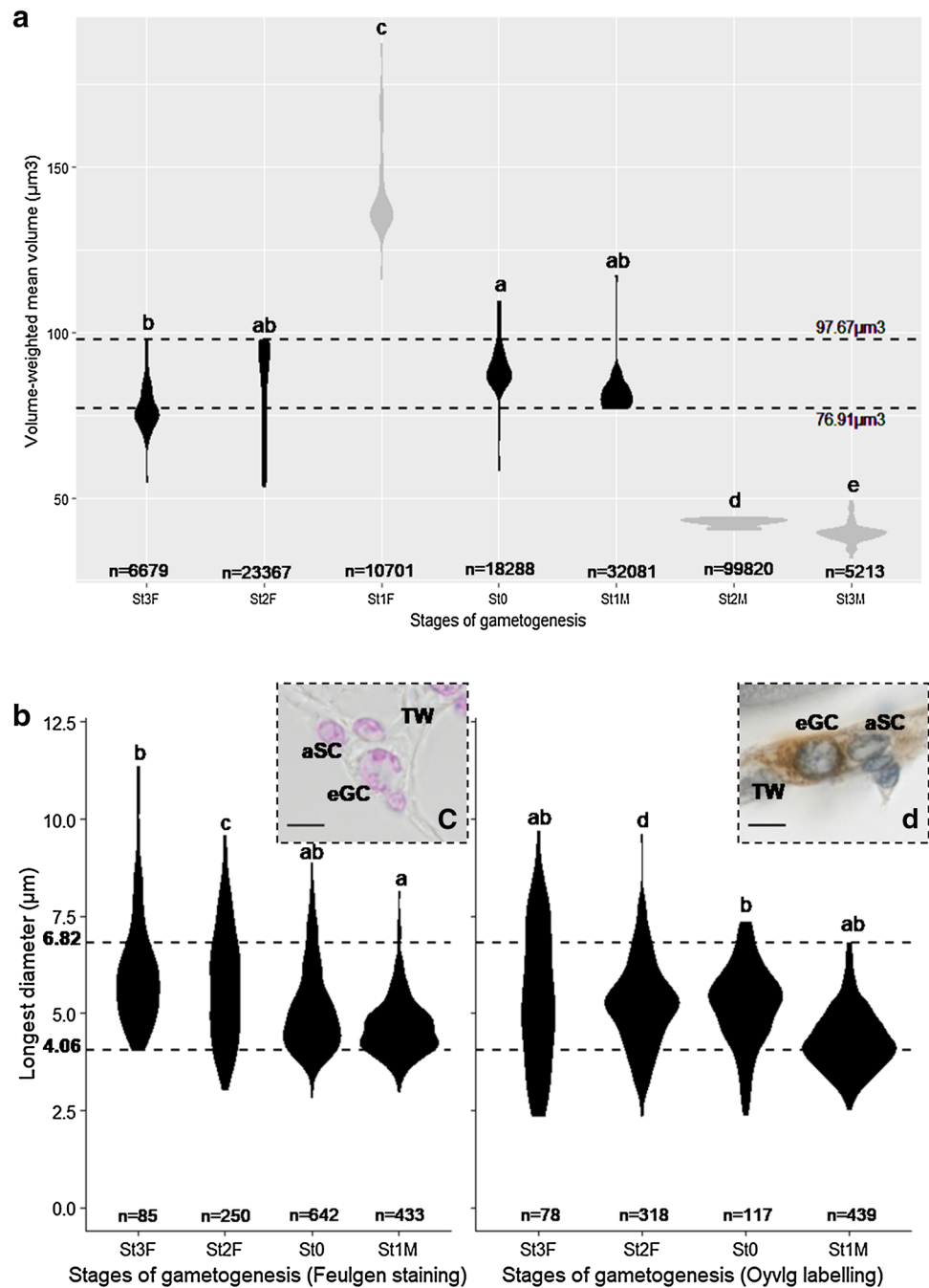
maturity stage (St3F). To characterize sub-populations of early germ cells, the second measurement step was conducted by studying only the four stages of interest mentioned above (Fig. 1b). For these four stages, the longest diameters of the nuclei of interest were measured first on the Feulgen stained slides and then on Oyvlg immunolabelled slides and further compared (Fig. 1b). The statistical analysis revealed that, for each stage, the nucleus measurements did not display any difference between Feulgen staining and Oyvlg immunolabelling, except in the gonial mitosis initiation stage in male. Moreover, no significant difference was found between the quiescence stage, the development and sexual maturity stages in female. The nuclei diameters shared in the four stages ranged from 4.06 to 6.82 μ m. Early germ cells presenting determined diameter were located along the tubule wall, presented a nucleus with slightly condensed chromatin (Fig. 1c) and an Oyvlg positive labelling (Fig. 1d), they were closely associated to a differentiated somatic cell (aSC) (Fig. 1c, d).

Nucleus elongation ratios (shortest diameter/longest diameter) of the early germ cell identified population were calculated for cells of interest stained with Feulgen or immunolabelled with Oyvlg. These elongation ratios ranged from 0.42 to 1 (Fig. 2). This result reflected that early germ cells present a round or irregular nucleus. To discriminate sub-populations in early germ cells, a coefficient of variation of 0.09 was calculated according to the evaluation of measurements reproducibility. Using this coefficient, we distinguished two sub-populations of early germ cells depending on their nucleus elongation ratios. The first sub-population presented round nuclei with an elongation ratio that is strictly superior to 0.8 and corresponded to 73% of the total early germ cells population. The second sub-population of early germ cells presented irregular nuclei with an elongation ratio equal or below to 0.8 and represented 27% of the total early germ cells population.

Oyvlg immunolabelling

Immunofluorescence detection using the Oyvlg antibody showed a specific signal in germ cells (Fig. 3). Cytoplasmic signal in germ cells was observed in the gonad through the reproductive cycle. During the quiescence stage, only large cells presenting an aspect of early germ cells were labelled (Fig. 3b). These cells are located along the wall of the tubule and present nuclei with slightly condensed chromatin underlined by DAPI staining (Fig. 3b inset). In the following stages of gonial mitosis initiation (Fig. 3c, male and Fig. 3d, female), germline development (Fig. 3e, male and Fig. 3f, female) and sexual maturity (Fig. 3g, male and Fig. 3h, female), Oyster Vasa positive labelling is observed only in early germ cells. It could be noted that the slight

Fig. 1 Graphical representation of the two-step histological quantitative approach. **a** Step 1 of the quantitative approach led us to estimate the volume-weighted mean volume of each field (75 fields per gametogenesis stage). The common population at the most stages of gametogenesis (four stages, colored in black) is represented by the dotted lines. **b** Step 2 of the quantitative histology led us to measure the longest diameter of each nucleus of interest on the four selected stages of gametogenesis (*St0* quiescence stage, *St1M* male gonial mitosis initiation stage, *St2F* female development stage, *St3F* female sexual maturity stage). The longest diameters of nucleus measured after Feulgen staining are represented on the left-end side of the figure and those measured after Oyvlg immunolabelling are represented on the right-end side of the figure. The common nucleus population in both Feulgen staining and Oyvlg immunodetection is represented by the dotted lines. The letters indicate the significant differences; the number of cells measured is annotated (n). Insets **c** (Feulgen staining) and **d** (Oyvlg immunodetection): Aspect of early germ cells belonging to the common population. Tubule wall (TW), early germ cell (eGC) and associated somatic cell (aSC). Scale bars: 5 μm (c, d)



staining observed in DAB immunolabelling around GSC was not noticed in immunofluorescence detection of Oyvlg.

Oyvlg expression

qPCR data showed that oyvlg transcript appears to be expressed throughout the gametogenesis for both male and female with significant increase correlated to the gametogenesis progress and with an expression that is significantly higher in the sexual maturity stage in female (Fig. 4a). To compare protein and transcript locations, in situ

hybridization was performed during the earliest stages of gametogenesis (Fig. 4b–d). Early germ cells were stained with the same pattern as Oyvlg protein expression labelling.

Germinal niche

The microenvironment or germinal niche of both types of early germ cells identified by quantitative histology was studied. At photonic scale, early germ cells appear to be closely surrounded by at least one associated somatic cell and are closed to a myoid cell (Fig. 5a). The associated

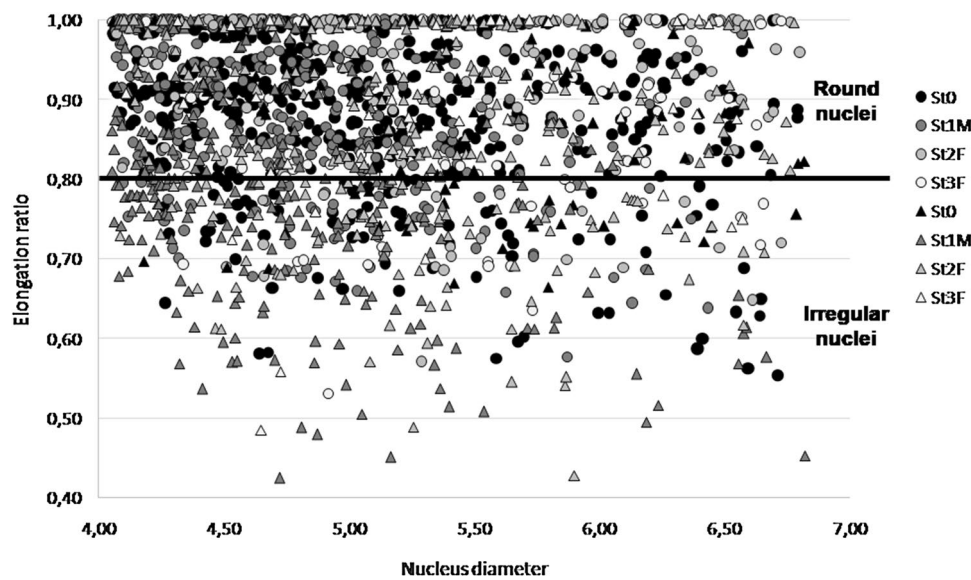


Fig. 2 Graphical representation of the elongation ratios for each nucleus diameter between 4.06 μm and 6.82 μm corresponding to the cell population of interest for the four gametogenesis stages selected (*St0* quiescence stage, *St1M* male gonial mitosis initiation stage, *St2F* female development stage, *St3F* female sexual maturity stage). The

elongation ratios obtained after Feulgen staining measurements are represented by circles and those obtained after Oyvlg immunolabelling measurements are represented by triangles. The elongation ratios that are strictly superior to 0.8 correspond to round nuclei while the elongation ratios that are below 0.8 correspond to irregular nuclei

somatic cells surrounding early germ cells are immunolabelled by a BMP2/4 antibody (Fig. 5b). Electron microscopy allowed to precise the structure of the germinal niche in oyster (Fig. 6). A continuum of the two types of early germ cells (with irregular or round nucleus) was observed several times in the gonadal tubule (Fig. 6a). Microenvironment of both early germ cell types (Fig. 6b, c) shared common elements: the location of early germ cell against the *basal lamina* near a myoid cell (Fig. 6d, e) and the presence of at least one closed associate somatic cell (Fig. 6f, g). Somatic cell associated with early germ cell sometimes contained some phagolysosomes in its cytoplasm (Fig. 6e). Both early germ cells types presented a nucleus with slightly condensed chromatin and a distinctive nuage in cytoplasm associated with numerous and round mitochondria (Fig. 6h, i). It has been noted that the early germ cells with round nucleus were quite often combined in two's or four's.

Finally, the distribution of the both types of early germ cells with round (Fig. 7a, b, red circles) and irregular (Fig. 7a, b, blue circles) nuclei was studied on a whole gonad section (whole slide image, WSI). Both early germ cells types are uniformly distributed in the oysters' gonad tubules, from the outer (against mantle) to the inner (against digestive area) parts of the gonad. The specificity of the vasa detection is evaluated by a negative control (Fig. 7c, d).

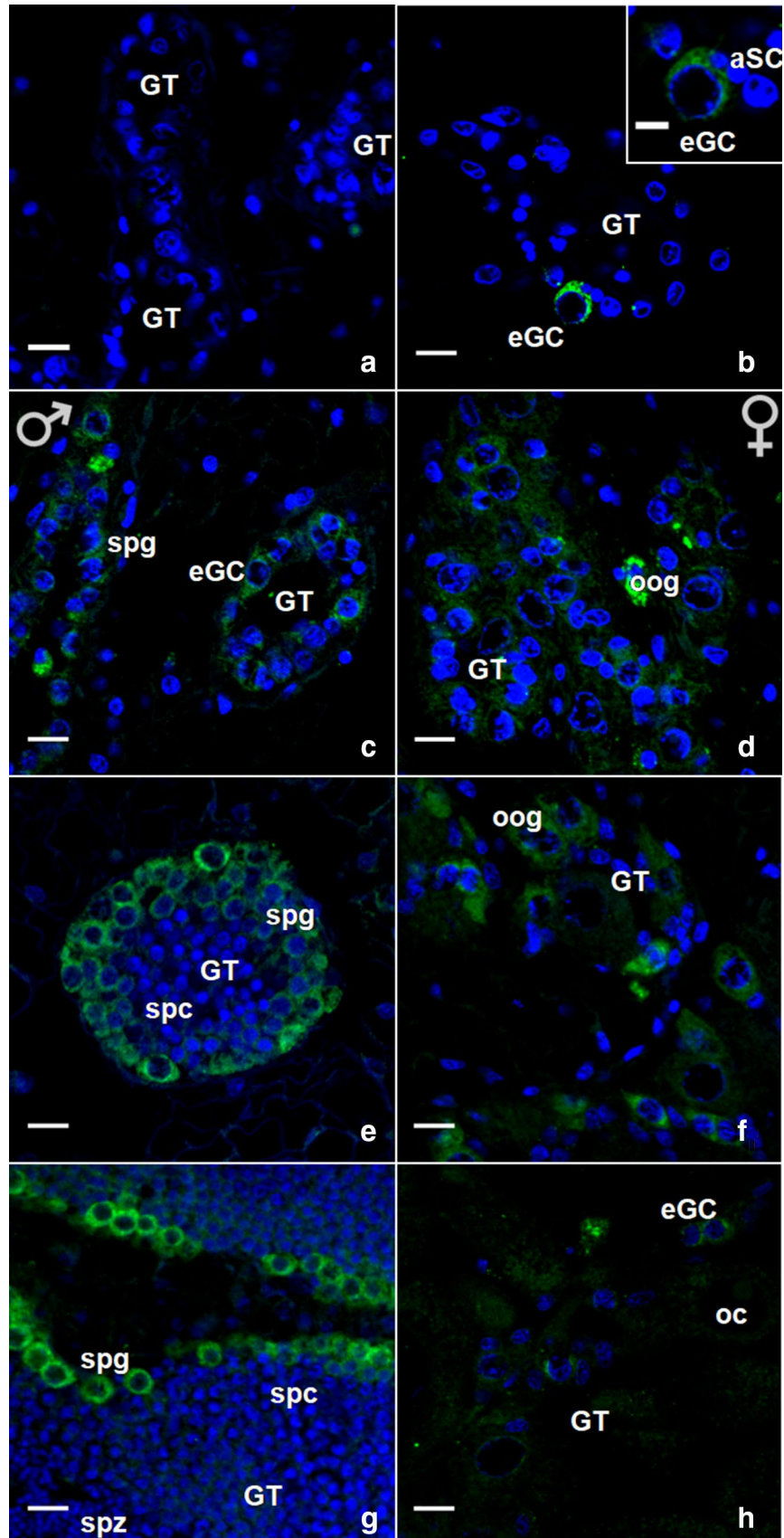
Discussion

The oyster *C. gigas* belongs to the lophotrochozoans, which presents very heterogeneous reproduction modes. In this alternative hermaphrodite, gonad cells (somatic and germ cells) are able to differentiate in female or male lines depending on the seasonal reproductive cycle. The germline is renewed each year and this study presents a quantitative and qualitative approach to better characterize the GSC in their niche in adult oyster. Previous studies carried out on the spermatogenesis of two molluscan species (*C. gigas* and *Mytilus galloprovincialis*) described two types of spermatogonia in the germinal epithelium (Franco et al. 2008; Prisco et al. 2017).

First, a population of early GC is identified in the oyster adult gonad

Germinal stem cells form a sustainable and scarce population that is common to all sexes and stages of *C. gigas*' reproductive cycle. The first result concerning the mean volume of the germ cells nuclei of interest revealed a common population of germ cells apparent in four stages of the gametogenesis: the quiescence stage, the gonial mitosis initiation stage in male, the developmental and

Fig. 3 Immunofluorescence detection of Oyvlg in male and female gonad tubules (GT) of *C. gigas* throughout the gametogenesis. **a** Negative control **b** Quiescence stage, few early germ cells (eGC) are positive to Oyvlg antibody and are found close to an associated somatic cell (aSC) (**b** inset). In male (**c, e, g**) and female (**d, f, h**) gametogenesis stages, Oyvlg immunodetection was restricted to germ cells. For gonial mitosis initiation (**c** male and **d** female), germline development (**e** male and **f** female) and sexual maturity stages (**g** male and **h** female), Oyvlg immunolabelling is observed from gonial to early oocytes and spermatocytes. Spermatogonia (spg), spermatocytes (spc) spermatozoa (spz), oogonia (oog) and oocyte (oc). Scale bars: 10 μ m (**a–h**) and 5 μ m (**b** inset)



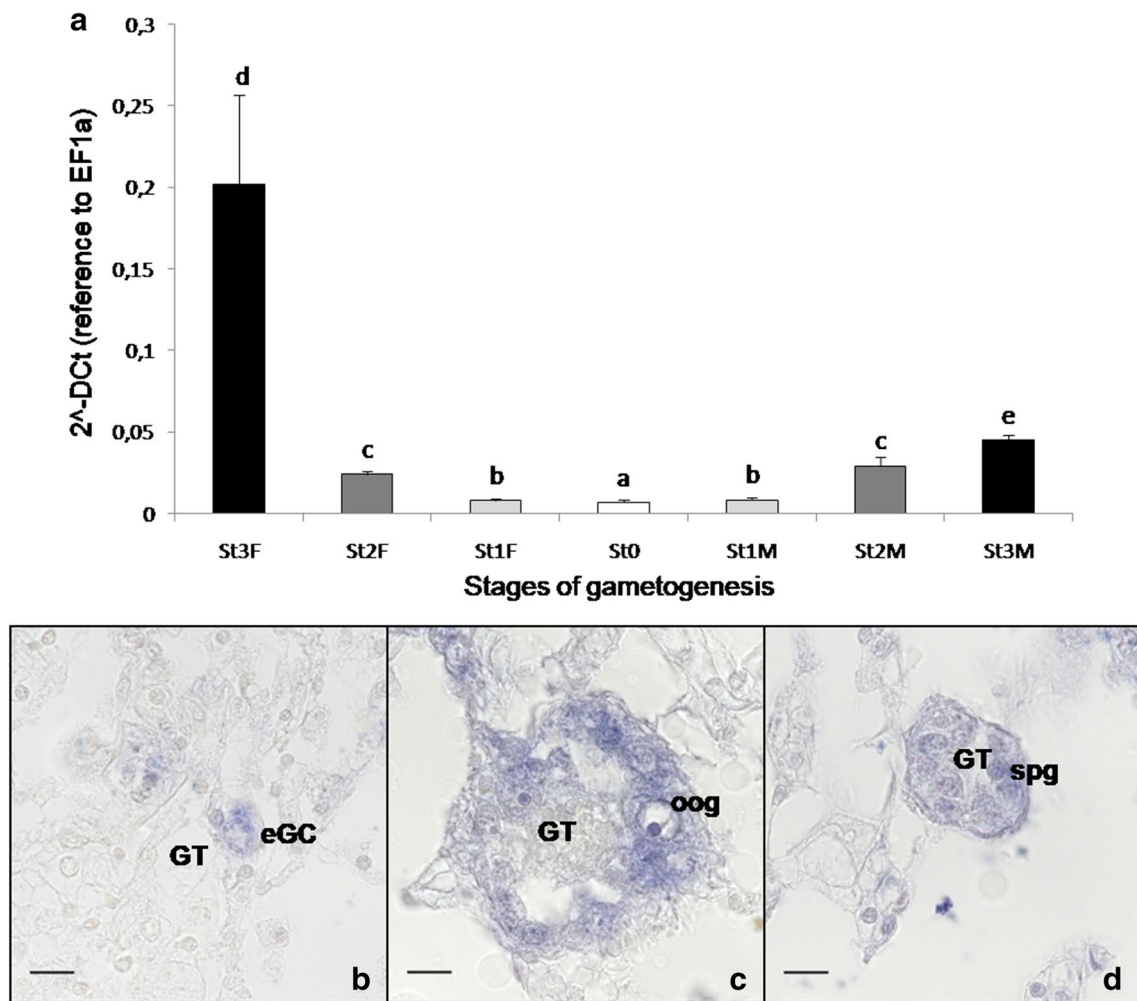


Fig. 4 Expression and location of *oylvg* transcript in *C. gigas*. **a** Quantification of *oylvg* transcript by qPCR at each stage of gametogenesis. Location of *oylvg* transcript in the *C. gigas* gonad tubules by in situ hybridization at the earliest stages of gametogenesis, the quiescent stage of gametogenesis (**b**), the gonial mitosis initiation stages in female (**c**) and male (**d**). *St0* quiescence stage, *St1F* and

M female and male gonial mitosis initiation stages, *St2F* and *2M* female and male development stages, *St3F* and *3M* female and male sexual maturity stages. Letters indicate significant differences. Gonad tubules (GT), early germ cells (eGC), oogonia (oog), spermatogonia (spg). Scale bars: 10 μm

Fig. 5 Characteristics of the early Germ Cells (eGC) and their microenvironment in *C. gigas*. **a** Feulgen staining of an early germ cell (eGC) closely related to an associated somatic cell (aSC) and a myoid cell (MC). **b** BMP2/4 immunodetection in the aSC cytoplasm in gonad tubules and negative control (inset). *eGC* early germ cell, *aSC* associated somatic cell, *MC* myoid cell, *TW* tubule wall, *GT* gonad tubule. Scale bars: 10 μm

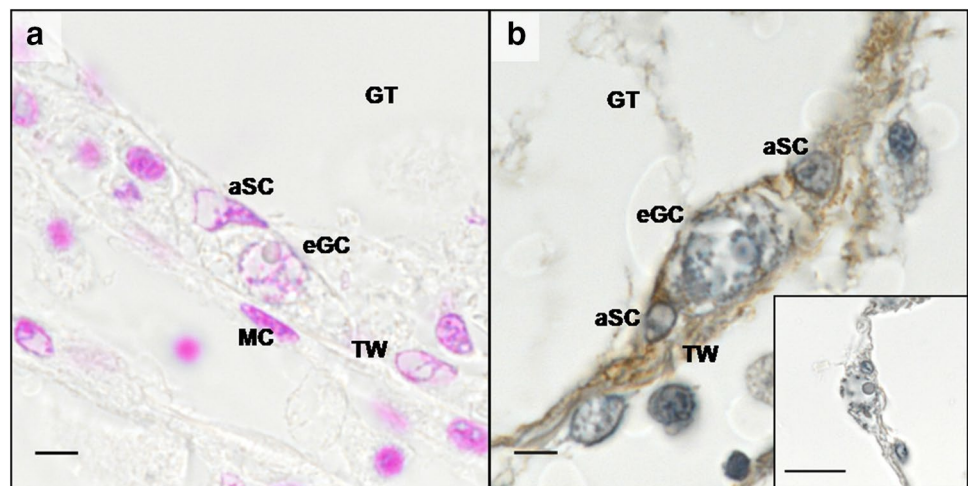


Fig. 6 Ultrastructural characteristics of the germinal niche in *C. gigas*. **a** Continuum of the two early germ cell (eGC) types in their microenvironment. **b** Ultrastructure of the niche of early germ cell with irregular nucleus (eGCir). **c** Ultrastructure of the microenvironment of early germ cell with round nucleus (eGCr). **d, e** Details of the basal lamina (BL) and the myoid cell (MC) of the microenvironment of both early germ cell types (irregular and round nucleus, respectively). **f, g** Characteristics of each associated somatic cell (aSC) observed. **h, i** Both early germ cells with irregular nucleus (eGCir) and early germ cells with round nucleus (eGCr) present a nuage (n) associated with numerous mitochondria (m). *eGCir* early germ cell with irregular nucleus, *eGCr* early germ cell with round nucleus, *aSC* associated somatic cell, *MC* myoid cell, *BL* basal lamina, *m* mitochondria, *n* nuage. Scale bars: 1 μm (**a–c**); 0.5 μm (**d–g**) and 0.2 μm (**h, i**)

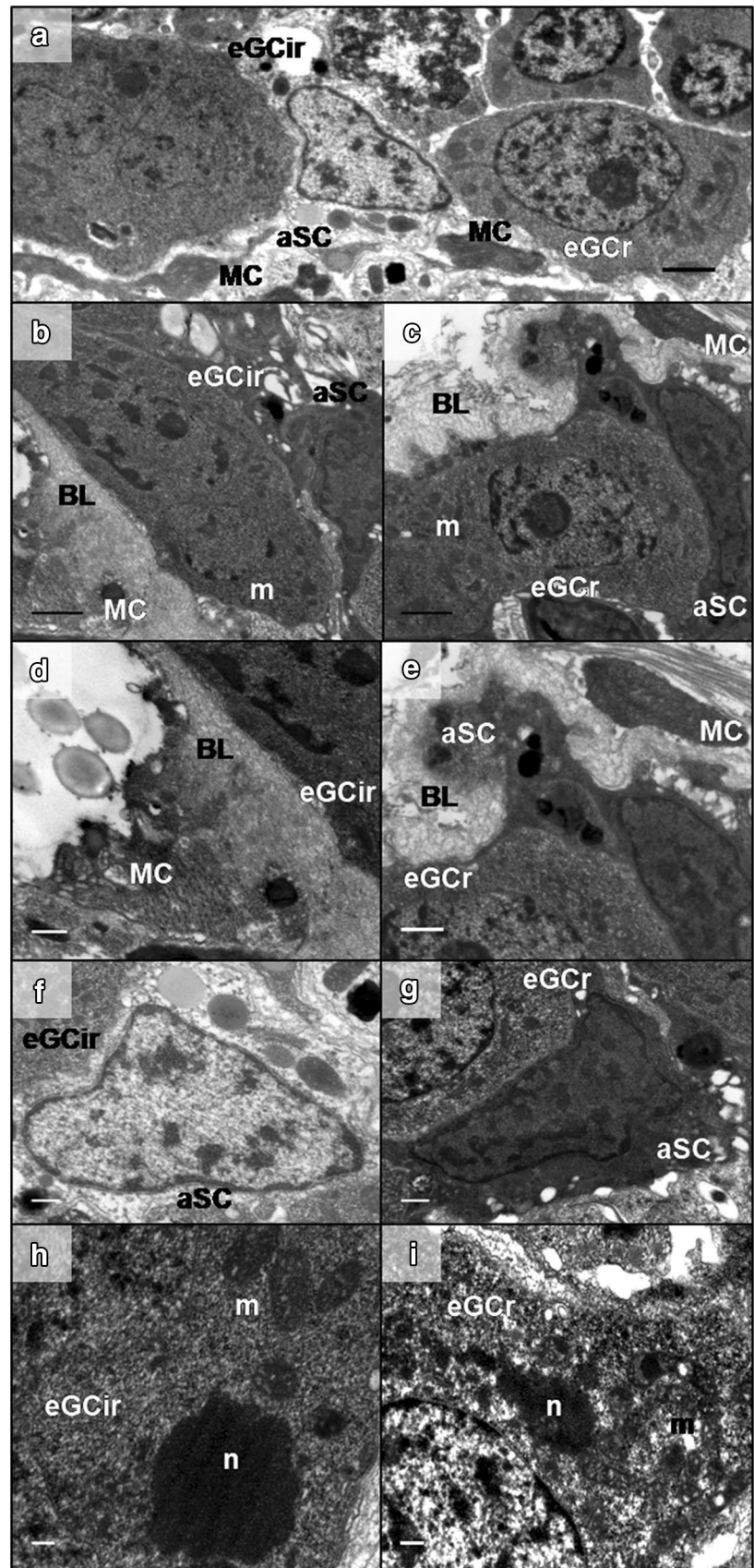
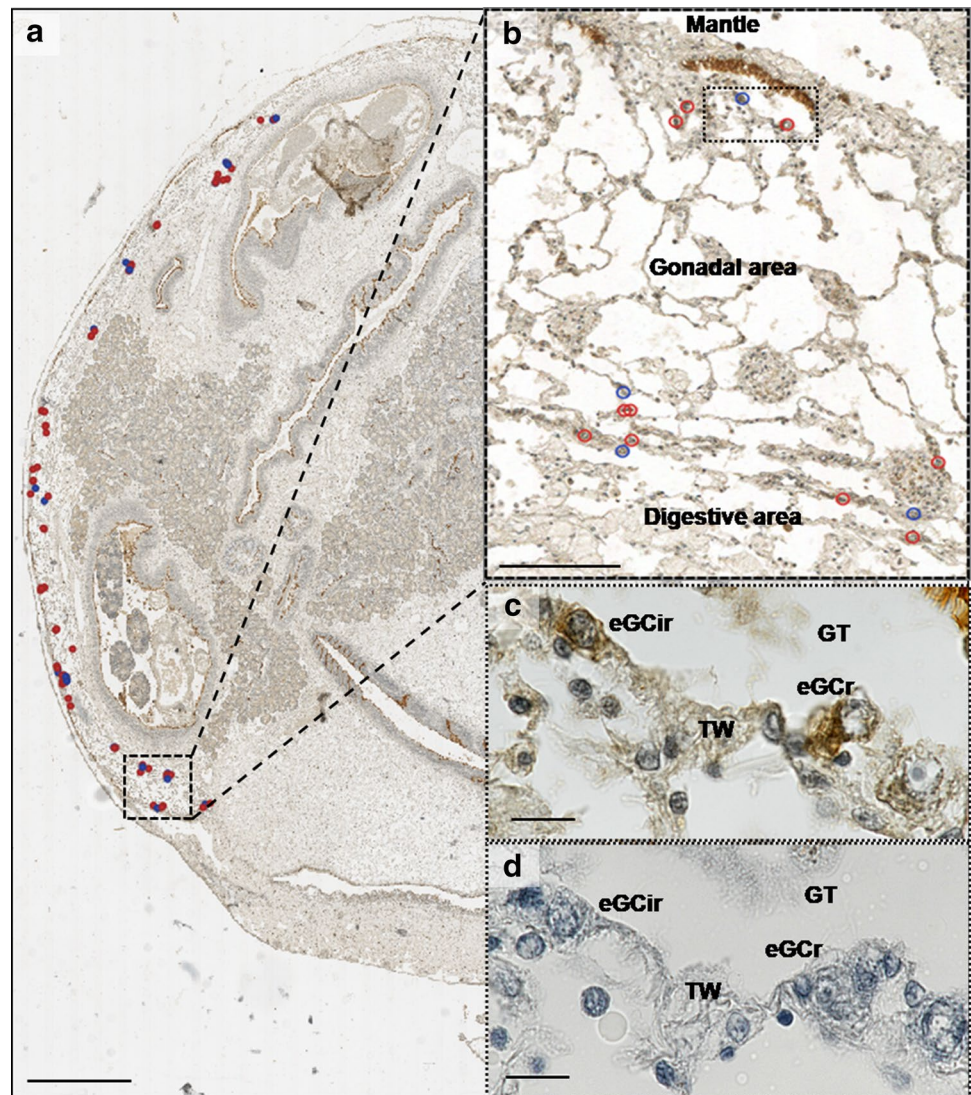


Fig. 7 Location of putative germinal niches in the gonad of *C. gigas*. **a** Whole slide image of Oyvlg labelling at the quiescence stage of gametogenesis (Stage 0). **b** Inset of the whole slide image. **c, d** Details and negative control of the dashed box area in the inset (magnification 100). Each putative germ stem cell belonging to the population of interest at this stage (nucleus diameter between 4.06 μm and 6.82 μm) are circled in the gonadal area. The red circles correspond to the round nuclei with an elongation ratio which is strictly superior to 0.8 and the blue circles represent the irregular nuclei with an elongation ratio below 0.8. *GT* gonad tubules, *TW* tubule wall, *pGSC* putative germ stem cell, *eGC* early germ cell. Scale bars: 1 mm (**a**), 0.1 mm (**b**) and 10 μm (**c, d**)



mature stages in female. The mean volumes obtained for this population of early germ cells nuclei are range from 76.91 to 97.67 μm^3 and might be partially consistent with a putative GSC type. The fact that we were unable to find any common cell nucleus diameters among all stages of gametogenesis is probably due to a technical bias. Indeed, we based our measures on a selection of cells presenting characteristics of early germ cells in each studied field. In the female, we probably selected young oogonia among the cells of interest, due to their position and low chromatin density. However, oogonia have larger nuclei leading to overestimation of mean volume. For male development and maturity stages, spermatogonia may be present among the considered cells of interest. These spermatogonia have a reduced nuclei (Franco et al. 2008) compared with early germ cells. This is why the quiescence stage, the male gonial mitosis initiation stage and the female development and maturity stages seem to be more relevant for the

further quantitative identification of the early germ cells in *C. gigas*.

Oyster vasa is expressed in the population of early germ cells

We performed Oyvlg immunodetection through the reproductive cycle to detect germinal cells in gonadal tubules. First detection of Oyvlg with DAB coloration showed a highly staining in early germ cells and a slight one just around them that could be due to a staining of associated somatic cells. However, the second immunodetection using fluorescence allowed us to conclude that Oyster Vasa positive labelling is exclusively observed in early germ cells, therefore, in the GSC. Recent data of Cavalier et al. (2017) report similar immunolabelling of Vasa in the oyster's gonad. In contrast, unlike Milani et al. (2017), we did not find any Vasa labelling in other tissues than in the gonad.

These differences between our study and the results previously obtained by Milani et al. might be due to differences in sensitivity of antibodies used. Indeed, the antibody used in our study is a *C. gigas* homologous Oyvlg antibody which links with different antigenic sequences than in Milani and collaborators' work. In complement, we noted that oylvlg transcript expression in germ cells was in accordance with the results obtained by Fabioux et al. (2004b). In our experiments, we noticed that at the quiescence stage, oylvlg transcript expression tends to appear in few germ cells. Oylvlg transcript expression increases during the gametogenesis course, probably because of the increasing amount of germ cells. Moreover, qPCR showed a peak of oylvlg expression at the female sexual maturity stage probably due to the oylvlg maternal mRNA accumulation. We noticed that vasa labelling is present in adult oyster gonad at all stages of gametogenesis that seek with a permanent gonad, germ line and GSC pool in adult in this species.

A common population of putative GSC is identified among early germ cells in male and female

For the four stages of gametogenesis (quiescence, male gonial mitosis initiation and female development and maturity stages) in which an early germ cells population was identified, we combined criteria of chromatin condensation, highlighted by Feulgen staining, and oyster Vasa immunodetection to identify putative GSC. The results confirmed the presence of a population of early germ cells that could be identified through some stemness criteria. The study of elongation ratios of nuclei in this population of early germ cells allowed us to identify two cell types, one presenting round nuclei (ratios strictly superior to 0.8) and the other with irregular nuclei (ratios equal or below to 0.8). An ultrastructural study showed that both early germ cells types present specific morphological criteria of GSC as a nucleus with slightly condensed chromatin and numerous grouped mitochondria close to a nuage structure in the cytoplasm. Both types are located against the *basal lamina*, are immunogold labelled by oyster Vasa (online resource 2) and their microenvironment consists in at least a closely associated somatic cell and a surrounding myoid cell. The only morphological difference found between the two types of early germ cells identified by the quantitative and molecular approaches is the shape of their nucleus (round or irregular). In the male, the two types of spermatogonia previously described in oyster present clearly round nuclei (Franco et al. 2008). Moreover, in tilapia, it has been shown that differentiated spermatogonia present a round nucleus while the undifferentiated spermatogonia of type A possesses an irregular nucleus well observed under electron microscopy but difficult to visualize under light microscopy (Schulz et al. 2010). In addition, in planarians, a group that is phylogenetically closely related to

the molluscan, the neoblasts, the stem cells able to differentiate in germ and somatic lines, present an irregular nucleus with slightly condensed chromatin becoming particularly apparent under transmission electron microscopy (Sato et al. 2006). All these elements enabled us to say that the identified early germ cells presenting an irregular nucleus correspond to the putative GSC in oyster and those presenting a round nucleus to the putative progenitors. This idea is supported by the more frequent observation of groups of putative progenitors (with round nucleus) in the tubule and by the fact that putative GSC (with irregular nucleus) represent only 27% of the total early germ cells population.

The germinal niche and its location are specified in the whole gonad

By the use of a heterologous antibody against BMP2/4, we observed the characteristics of a labelling specifically associated somatic cells closely related to the early germ cells identified. This result suggests the eventual involvement of TGF- β signaling pathway in the functioning of germinal niche in *C. gigas*. In *drosophila*, the TGF- β signal transduction pathway has been determined to impact the number of germline stem cells and the size of the stem cell niche (Schulz et al. 2004). Moreover Dpp, homologous of the human BMP2, well known for its implication in the germinal niche functioning in *D. melanogaster* (Xie and Spradling 1998), presents a strong homology with Cg-mGDF in *C. gigas* (Lelong et al. 2000; Fleury et al. 2008). Further studies are required to describe the proliferation and its regulation of identified putative GSC and progenitors in oyster. In addition, the somatic cells associated with the germline in oyster should be further studied to determine their functional features.

The study of the distribution of putative GSC on a Whole Slide Image (WSI) allowed us to conclude that the germinal niches in adult oyster are uniformly distributed on a gonad scale. The distribution of germinal niches in oyster from the first gametogenesis and the following ones could expand from the outermost part of the gonad (against the mantle) (Santerre et al. 2013; Cavelier et al. 2017) to the innermost part (against the digestive area).

Conclusions

Concerning the origin of GSC in *C. gigas* during development, the mRNA from the oyster vasa gene is found in vegetal pole of oocytes and becomes progressively restricted to the 4d blastomere. These two daughter cells persist without further proliferation during the subsequent larval stages and, are therefore, believed to be the PGC of *C. gigas* (Fabioux et al. 2004a). Concerning Cg-Nanos-like, transcripts

were also localized in the vegetal pole of oocytes but are uniformly expressed at early cleavage stages and appear restricted to two cells clusters at gastrulation until umbo-larvae which could be the putative PGC (Xu et al. 2018). Classically, after their migration in the pre-adult gonad, PGC with niche cellular components become GSC which become differentiated germ cells during gametogenesis (Saffman and Lasko 1999).

However, the issue of the nature of stem cells and the renewal of the somatic and germlines at each reproductive cycle remains open in *C. gigas*. Two scenarios should be taken into account. The first one consists on the persistence of a single stem cell able to give rise of both somatic and germinal lineages in the adult gonad, which could be in accordance with the definition of primordial stem cells (PriSC) of Solana (2013). In this case, our study identified a putative GSC that could derive from this single stem cell still unidentified in our work. The second possibility considers that the PGC in oyster are strictly germinal and become GSC at the first gametogenesis in adult. In this case, we characterised in our study the putative GSC in adult oyster and the somatic stem cell at the origin of the intragonadal somatic line is yet to be identified. The use of complementary conserved markers of stemness and GSC in *C. gigas* (for example KLF, Piwi, Nanos) could allow identifying cells to validate one or other of these possibilities.

Acknowledgements PhD of M. Cherif-Feildel was financially supported by the French Research Minister (PhD grant). The authors are grateful to C. Fabioux (Université de Bretagne occidentale, Institut universitaire européen de la mer, LEMAR) and C. Corporeau (Ifremer, LPI) for the oyster vasa antibody supplying. The authors thank J.P. Robin for essential advice on all the statistical aspects of this study. Proofreading of English text has been realised by C. Quint of the translation centre of the Carré international UNICAEN.

Compliance with ethical standards

Conflict of interest The authors declare no competing financial interests.

References

- Adoutte A, Balavoine G, Lartillot N, Lespinet O, Prud'homme B, de Rosa R (2000) The new animal phylogeny: reliability and implications. *Proc Natl Acad Sci USA* 97:4453–4456. <https://doi.org/10.1073/pnas.97.9.4453>
- Baguñà J (2012) The planarian neoblast: the rambling history of its origin and some current black boxes. *Int J Dev Biol* 56:19–37. <https://doi.org/10.1387/ijdb.113463jb>
- Bankhead P, Loughrey MB, Fernández JA, Dombrowski Y, McArt DG, Dunne PD, McQuaid S, Gray RT, Murray LJ, Coleman HG, James JA, Salto-Tellez M, Hamilton PW (2017) QuPath: open source software for digital pathology image analysis. *Sci Rep* 7:1–7. <https://doi.org/10.1038/s41598-017-17204-5>
- Berthelin C, Kellner K, Mathieu M (2000a) Histological characterization and glucose incorporation into glycogen of the Pacific oyster *Crassostrea gigas* storage cells. *Mar Biotechnol* 2:136–145. <https://doi.org/10.1007/s101269900017>
- Berthelin C, Kellner K, Mathieu M (2000b) Storage metabolism in the Pacific oyster (*Crassostrea gigas*) in relation to summer mortalities and reproductive cycle (West Coast of France). *Comp Biochem Physiol B Biochem Mol Biol* 125:359–369. [https://doi.org/10.1016/S0305-0491\(99\)00187-X](https://doi.org/10.1016/S0305-0491(99)00187-X)
- Brown DL (2017) Bias in image analysis and its solution: unbiased stereology. *J Toxicol Pathol* 30:183–191. <https://doi.org/10.1293/tox.2017-0013>
- Brown FD, Swalla BJ (2012) Evolution and development of budding by stem cells: Ascidian coloniality as a case study. *Dev Biol* 369:151–162. <https://doi.org/10.1016/j.ydbio.2012.05.038>
- Cavelier P, Cau J, Morin N, Delsert C (2017) Early gametogenesis in the Pacific oyster: new insights using stem cell and mitotic markers. *J Exp Biol*. <https://doi.org/10.1242/jeb.167734>
- Chiari-Garcia H, Russell LD (2001) High-resolution light microscopic characterization of mouse spermatogonia. *Biol Reprod* 65:1170–1178
- Chiari-Garcia H, Russell LD (2002) Ultrastructure cellulaire et tissulaire. *Approch Reprod* 123:567–577. <https://doi.org/10.1530/rep.0.1230567>
- Chong T, Stary JM, Wang Y, Newmark P (2011) Molecular markers to characterize the hermaphroditic reproductive system of the planarian Schmidtea mediterranea. *BMC Dev Biol* 11:69. <https://doi.org/10.1186/1471-213X-11-69>
- Cruz-Orive L-M, Hunziker EB (1986) Stereology for anisotropic cells: application to growth cartilage. *J Microsc* 143:47–80. <https://doi.org/10.1111/j.1365-2818.1986.tb02765.x>
- Dheilly NM, Lelong C, Huvet A, Favrel P (2011) Development of a Pacific oyster (*Crassostrea gigas*) 31,918-feature microarray: identification of reference genes and tissue-enriched expression patterns. *BMC Genom* 12:468. <https://doi.org/10.1186/1471-2164-12-468>
- Dheilly NM, Lelong C, Huvet A, Kellner K, Dubos M-P, Riviere G, Boudry P, Favrel P (2012) Gametogenesis in the Pacific oyster *Crassostrea gigas*: a microarrays-based analysis identifies sex and stage specific genes. *PLoS One* 7:e36353. <https://doi.org/10.1371/journal.pone.0036353>
- Dubos MP, Bernay B, Favrel P (2016) Molecular characterization of an adipokinetic hormone-related neuropeptide (AKH) from a mollusk. *Gen Comp Endocrinol* 243:15–21. <https://doi.org/10.1016/j.ygcen.2016.11.002>
- Fabioux C, Huvet A, Lelong C, Robert R, Pouvreau S, Daniel J, Minguant C, Le Pennec M (2004a) Oyster vasa-like gene as a marker of the germline cell development in *Crassostrea gigas*. *Biochem Biophys Res Commun* 320:592–598. <https://doi.org/10.1016/j.bbrc.2004.06.009>
- Fabioux C, Pouvreau S, Le Roux F, Huvet A (2004b) The oyster vasa-like gene: a specific marker of the germline in *Crassostrea gigas*. *Biochem Biophys Res Commun* 315:897–904. <https://doi.org/10.1016/j.bbrc.2004.01.145>
- Fabioux C, Corporeau C, Quillien V, Favrel P, Huvet A (2009) In vivo RNA interference in oyster-vasa silencing inhibits germ cell development. *FEBS J* 276:2566–2573. <https://doi.org/10.1111/j.1742-4658.2009.06982.x>
- Ferraro F, Lo Celso C, Scadden D (2010) Adult stem cells and their niches. *Adv Exp Med Biol* 695:155–168. <https://doi.org/10.1007/978-1-4419-7037-4>
- Fleury E, Fabioux C, Lelong C, Favrel P, Huvet A (2008) Characterization of a gonad-specific transforming growth factor- β superfamily member differentially expressed during the reproductive cycle of the oyster *Crassostrea gigas*. *Gene* 410:187–196

- Franco A, Heude Berthelin C, Goux D, Sourdain P, Mathieu M (2008) Fine structure of the early stages of spermatogenesis in the Pacific oyster, *Crassostrea gigas* (Mollusca, Bivalvia). *Tissue Cell* 40:251–260. <https://doi.org/10.1016/j.tice.2007.12.006>
- Franco A, Jouaux A, Mathieu M, Sourdain P, Lelong C, Kellner K, Heude Berthelin C (2010) Proliferating cell nuclear antigen in gonad and associated storage tissue of the Pacific oyster *Crassostrea gigas*: seasonal immunodetection and expression in laser microdissected tissues. *Cell Tissue Res* 340:201–210. <https://doi.org/10.1007/s00441-009-0923-6>
- Gabe M (1968) *Techniques histologiques*, 6th edn. Masson, Paris
- Garcia Y, Breen A, Burugapalli K, Dockery P, Pandit A (2007) Stereological methods to assess tissue response for tissue-engineered scaffolds. *Biomaterials* 28:175–186. <https://doi.org/10.1016/j.biomaterials.2006.08.037>
- Golub VM, Brewer J, Wu X, Kuruba R, Short J, Manchi M, Swonke M, Younus I, Reddy DS (2015) Neurostereology protocol for unbiased quantification of neuronal injury and neurodegeneration. *Front Aging Neurosci* 7:1–14. <https://doi.org/10.3389/fnagi.2015.00196>
- Gundersen H, Jensen E (1985) Stereological estimation of the volume-weighted mean volume of arbitrary particles observed on random sections. *J Microsc* 138:127–142. <https://doi.org/10.1111/j.1365-2818.1985.tb02607.x>
- Herpin A, Lelong C, Favrel P (2004) Transforming growth factor- β -related proteins: an ancestral and widespread superfamily of cytokines in metazoans. *Dev Comp Immunol* 28:461–485. <https://doi.org/10.1016/j.dci.2003.09.007>
- Herpin A, Lelong C, Becker T, Rosa F, Favrel P, Cunningham C (2005) Structural and functional evidence for a singular repertoire of BMP receptor signal transducing proteins in the lophotrochozoan *Crassostrea gigas* suggests a shared ancestral BMP/activin pathway. *FEBS J* 272:3424–3440. <https://doi.org/10.1111/j.1742-4658.2005.04761.x>
- Heude Berthelin C, Laisney J, Espinosa J, Martin O, Hernandez G, Mathieu M, Kellner K (2001) Storage and reproductive strategy in *Crassostrea gigas* from two different growing areas (Normandy and the Atlantic coast, France). *Invertebr Reprod Dev* 40:79–86. <https://doi.org/10.1080/07924259.2001.9652500>
- Huvet A, Fleury E, Corporeau C, Quillien V, Daniel JY, Riviere G, Boudry P, Fabioux C (2012) In vivo RNA interference of a gonad-specific transforming growth factor- β in the Pacific oyster *Crassostrea gigas*. *Mar Biotechnol* 14:402–410. <https://doi.org/10.1007/s10126-011-9421-4>
- Jagut M, Huynh JR (2007) Régulation des cellules souches de la lignée germinale. *Med Sci*. <https://doi.org/10.1051/medsci/20072367611>
- Jemaà M, Morin N, Cavelier P, Cau J, Strub JM, Delsert C (2014) Adult somatic progenitor cells and hematopoiesis in oysters. *J Exp Biol* 217:3067–3077. <https://doi.org/10.1242/jeb.106575>
- Johnson L, Thompson DL, Varner DD (2008) Role of Sertoli cell number and function on regulation of spermatogenesis. *Anim Reprod Sci* 105:23–51. <https://doi.org/10.1016/j.anireprosci.2007.11.029>
- Jouaux A, Heude Berthelin C, Sourdain P, Mathieu M, Kellner K (2010) Gametogenic stages in triploid oysters *Crassostrea gigas*: Irregular locking of gonial proliferation and subsequent reproductive effort. *J Exp Mar Bio Ecol* 395:162–170. <https://doi.org/10.1016/j.jembe.2010.08.030>
- Juliano CE, Swartz SZ, Wessel GM (2010) A conserved germline multipotency program. *Development* 137:4113–4126. <https://doi.org/10.1242/dev.047969>
- Ladekarl M (1998) Objective malignancy grading: a review emphasizing unbiased stereology applied to breast tumors. *APMIS Suppl* 79:1–34
- Lasko P (2013) The DEAD-box helicase vasa: evidence for a multiplicity of functions in RNA processes and developmental biology. *Biochim Biophys Acta Gene Regul Mech* 1829:810–816. <https://doi.org/10.1016/j.bbagr.2013.04.005>
- Le Quere H, Herpin A, Huvet A, Lelong C, Favrel P (2009) Structural and functional characterizations of an Activin type II receptor orthologue from the Pacific oyster *Crassostrea gigas*. *Gene* 436:101–107. <https://doi.org/10.1016/j.gene.2009.01.010>
- Lelong C, Mathieu M, Favrel P (2000) Structure and expression of mGDF, a new member of the transforming growth factor-beta superfamily in the bivalve mollusc *Crassostrea gigas*. *Eur J Biochem* 267:3986–3993. <https://doi.org/10.1046/j.1432-1327.2000.01432.x>
- Maceren-Pates M, Kurita Y, Pates G, Yoshikuni M (2015) A model for germ cell development in a fully segmented worm. *Zool Lett* 1:34. <https://doi.org/10.1186/s40851-015-0035-y>
- Meijer GA, Baak JPA, Talbot IC, Atkin WS, Meuwissen SGM (1998) Predicting the risk of metachronous colorectal cancer in patients with rectosigmoid adenomas using quantitative pathological features. A case-control study. *J Pathol* 184:63–70
- Milani L, Maurizii MG, Pecci A, Ghiselli F, Passamonti M (2015) Localization and dynamics of primordial germ cells in the bivalve species *Ruditapes philippinarum*. *Mol Reprod Dev* 82:406–407. <https://doi.org/10.1002/mrd.22502>
- Milani L, Pecci A, Ghiselli F, Passamonti M, Bettini S, Franceschini V, Maurizii MG (2017) VASA expression suggests shared germ line dynamics in bivalve molluscs. *Histochem Cell Biol* 148:157–171. <https://doi.org/10.1007/s00418-017-1560-x>
- Morrison SJ, Spradling AC (2008) Stem cells and niches: mechanisms that promote stem cell maintenance throughout life. *Cell* 132:598–611. <https://doi.org/10.1016/j.cell.2008.01.038>
- Newmark PA, Alvarado AS (2000) Bromodeoxyuridine specifically labels the regenerative stem cells of planarians. *Dev Biol* 220:142–153. <https://doi.org/10.1006/dbio.2000.9645>
- Obata M, Sano N, Kimata S, Nagasawa K, Yoshizaki G, Komaru A (2010) The proliferation and migration of immature germ cells in the mussel, *Mytilus galloprovincialis*: observation of the expression pattern in the *M. galloprovincialis* vasa-like gene (Myvlg) by in situ hybridization. *Dev Genes Evol* 220:139–149. <https://doi.org/10.1007/s00427-010-0335-3>
- Prisco M, Agnese M, De Marino A, Andreuccetti P, Rosati L (2017) Spermatogenic cycle and steroidogenic control of spermatogenesis in *Mytilus galloprovincialis* collected in the bay of Naples. *Anat Rec* 300:1881–1894. <https://doi.org/10.1002/ar.23626>
- Rink JC (2013) Stem cell systems and regeneration in planaria. *Dev Genes Evol* 223:67–84. <https://doi.org/10.1007/s00427-012-0426-4>
- Rossi L, Salvetti A, Batistoni R, Deri P, Gremigni V (2008) Planarians, a tale of stem cells. *Cell Mol Life Sci* 65:16–23. <https://doi.org/10.1007/s00018-007-7426-y>
- Saffman EEF, Lasko P (1999) Germline development in vertebrates and invertebrates. *Cell Mol Life Sci* 55:1141–1163. <https://doi.org/10.1007/s000180050363>
- Santerre C, Sourdain P, Marc N, Mingant C, Robert R, Martinez A (2013) Oyster sex determination is influenced by temperature—First clues in spat during first gonadic differentiation and gametogenesis. *Comp Biochem Physiol Part A* 165:61–69. <https://doi.org/10.1016/j.cbpa.2013.02.007>
- Sato K, Shibata N, Orii H, Amikura R, Sakurai T, Agata K, Kobayashi S, Watanabe K (2006) Identification and origin of the germline stem cells as revealed by the expression of nanos-related gene in planarians. *Dev Growth Differ* 48:615–628. <https://doi.org/10.1111/j.1440-169X.2006.00897.x>
- Scadden DT (2006) The stem-cell niche as an entity of action. *Nature* 441:1075–1079. <https://doi.org/10.1038/nature04957>
- Schmitz C, Hof PR (2005) Design-based stereology in neuroscience. *Neuroscience* 130:813–831. <https://doi.org/10.1016/j.neurosci.2004.08.050>

- Schulz C, Kiger AA, Tazuke SI, Yamashita YM, Pantalena-Filho LC, Jones DL, Wood CG, Fuller MT (2004) A misexpression screen reveals effects of bag-of-marbles and TGF β class signaling on the *Drosophila* male germ-line stem cell lineage. *Genetics* 167:707–723. <https://doi.org/10.1534/genetics.103.023184>
- Schulz RW, de França LR, Lareyre JJ, LeGac F, Chiarini-Garcia H, Nobrega RH, Miura T (2010) Spermatogenesis in fish. *Gen Comp Endocrinol* 165:390–411. <https://doi.org/10.1016/j.ygcen.2009.02.013>
- Silva RC, Costa GMJ, Andrade LM, França LR (2010) Testis stereology, seminiferous epithelium cycle length, and daily sperm production in the ocelot (*Leopardus pardalis*). *Theriogenology* 73:157–167. <https://doi.org/10.1016/j.theriogenology.2009.08.009>
- Solana J (2013) Closing the circle of germline and stem cells: the primordial stem cell hypothesis. *Evodevo* 4:2. <https://doi.org/10.1186/2041-9139-4-2>
- Spradling A, Fuller MT, Braun RE, Yoshida S (2011) Germline stem cells. *Cold Spring Harb Perspect Biol* 3:1–20. <https://doi.org/10.1101/cshperspect.a002642>
- Steele S, Mulcahy M (1999) Gametogenesis of the oyster *Crassostrea gigas* in southern Ireland. *J Mar Biol Ass UK* 79:673–686. <https://doi.org/10.1017/S0025315498000836>
- Xie T, Spradling AC (1998) Decapentaplegic is essential for the maintenance and division of germline stem cells in the *Drosophila* ovary. *Cell* 94:251–260. [https://doi.org/10.1016/S0092-8674\(00\)81424-5](https://doi.org/10.1016/S0092-8674(00)81424-5)
- Xu R, Li Q, Yu H, Kong L (2018) Oocyte maturation and origin of the germline as revealed by the expression of Nanos-like in the Pacific oyster *Crassostrea gigas*. 663:41–50. <https://doi.org/10.1016/j.gene.2018.04.021>
- Zhang G, Fang X, Guo X, Li L, Luo R, Xu F, Yang P, Wang J, Zhang L, Wang X, Qi H, Xiong Z, Que H, Xie Y, Holland PWH, Paps J, Zhu Y, Wu F, Chen Y, Wang J, Peng C, Meng J, Yang L, Liu J, Wen B, Zhang N, Huang Z, Zhu Q, Feng Y, Mount A, Hedgecock D, Xu Z, Liu Y, Domazet-Lošo T, Du Y, Sun X, Zhang S, Liu B, Cheng P, Jiang X, Li J, Fan D, Wang W, Fu W, Wang T, Wang B, Zhang J, Peng Z, Li Y, Li N, Wang J, Chen M, He Y, Tan F, Song X, Zheng Q, Huang R, Yang H, Du X, Chen L, Yang M, Gaffney PM, Wang S, Luo L, She Z, Ming Y, Huang W, Zhang S, Huang B, Zhang Y, Qu T, Ni P, Miao G, Wang J, Wang Q, Steinberg CEW, Wang H, Li N, Qian L, Zhang G, Li Y, Yang H, Liu X, Yin Y, Wang J (2012) The oyster genome reveals stress adaptation and complexity of shell formation. *Nature* 490:49–54. <https://doi.org/10.1038/nature11413>
- Zhang L, Li L, Guo X, Litman GW, Dishaw LJ, Zhang G (2015) Massive expansion and functional divergence of innate immune genes in a protostome. *Sci Rep* 5:1–11. <https://doi.org/10.1038/srep08693>
- Zhao X, Yu H, Kong L, Li Q (2012) Transcriptomic responses to salinity stress in the Pacific oyster *Crassostrea gigas*. *PLoS One*. <https://doi.org/10.1371/journal.pone.0046244>